Bacterial infection microenvironment-responsive enzymatically degradable multilayer films for multifunctional antibacterial properties

Article *in* Journal of Materials Chemistry B · October 2017

DOI: 10.1039/C7TB02114C

Qingqing Yao
Xiamen University

Yi Wang
Wenzhou Institute of Biomaterials and Engineering

Jian Ji
Zhejiang University

Hao Chen
Chinese Culture University

Journal of Materials Chemistry B

Accepted Manuscript

View Article Online
DOI: 10.1039/C7TB02114C

Bacterial infection microenvironment-responsive enzymatically degradable multilayer films for multifunctional antibacterial properties

Qingqing Yao[a, b], Zi Ye[a], Lin Sun[a], Yingying Jin[a], Qingwen Xu[a], Mei Yang[a], Yi Wang[b], Yunlong Zhou[b], Jian Ji[c], Hao Chen[a, b*], and Bailiang Wang[a, b*]

[a]School of Ophthalmology & Optometry, Eye Hospital, Wenzhou Medical University, Wenzhou, 325027, China

[b]Wenzhou Institute of Biomaterials and Engineering, Chinese Academy of Sciences, Wenzhou, 32500, China

[c]MOE Key Laboratory of Macromolecule Synthesis and Functionalization, Department of Polymer Science and Engineering, Zhejiang University, Hangzhou 310027, China

* Corresponding author. Fax: +86 577 88017524.

E-mail: chenhao@mail.eye.ac.cn (H. Chen); wangbailiang2006@aliyun.com (B.L. Wang)

Abstract:

The adhesion of bacteria is one of the most important stages in biofilm formation and bacterial infection. Once bacteria have adhered to a biomaterial surface, it is hard to eliminate them and bacterial growth and infection are inevitable. In the current study, we have designed and constructed enzymatically degradable (hyaluronic acid/chitosan)$_n$-(hyaluronic acid/ polylysine)$_n$ ((HA/CHI)$_n$-(HA/PLL)$_n$) composite multilayer films *via* a layer-by-layer self-assembly method. Spectroscopic ellipsometry and scanning electron microscopy cross section measurements showed the exponential growth behavior of the (HA/CHI)$_{10}$-(HA/PLL)$_{10}$ multilayer films (~2 μm). The increased secretion of hyaluronidase and chymotrypsin in the bacterial infection microenvironment led to the fast degradation of the outer (PLL/HA)$_n$ multilayer films in the first 24 h. Enzymatic degradation of the multilayer films efficiently reduced both *Staphylococcus aureus* and *Escherichia coli* adhesion (>99%). Bacterial LIVE/DEAD staining demonstrated the bactericidal action of the remaining bottom (CHI/HA)$_n$ multilayer films against the two kinds of bacteria. *In vivo* subcutaneous tests in New Zealand white rabbits, wound appearance and histopathology analysis showed that the implantation of composite multilayer film-modified PDMS promoted wound healing and the materials demonstrated a self-defense antibacterial effect. The material demonstrated both anti-adhesive and bactericidal properties and could be used to modify biomedical implants.

Keywords: Bacterial infections; microenvironment; enzymatic degradation; multilayer films; antibacterial

1. Introduction

Biomaterial-related infections contribute to approximately 64% of the hospital acquired infections globally, among which biofilm formation on biomaterial surfaces represents the majority of the infections [1, 2]. The bacteria in dense biofilms are up to 1000 times more resistant to antibiotics, compared with the resistance of planktonic bacteria, and this resistance is conferred through gene transfer and configuration changes [3, 4]. Furthermore, contaminated implants must be extracted and

View Article Online
DOI: 10.1039/C7TB02114C

replaced because of the lack of treatment techniques against biofilms and implant infections. More than 100,000 people die from infections related to biomedical implants each year in the United States.

The development of bacterial infections can be divided into three stages: bacterial adhesion, bacterial growth and biofilm formation, among which bacterial adhesion is the first and most crucial stage [5-7]. Once bacterial adhesion becomes irreversible, biofilm formation and bacterial infections are inevitable [8-10]. To date, many kinds of antibacterial surfaces, including those incorporating conventional anti-adhesive/anti-fouling properties [11, 12], bactericidal properties [13, 14] and the release of antibacterial agents [15, 16], have been developed to reduce the incidence of infection. However, it is difficult for antibacterial surfaces with just one type of antibacterial property to produce ideal and long-term efficacy [17-19]. For example, hydrophilic coatings (such as polyethylene glycol, polyvinyl alcohol, and polyvinylpyrrolidone) can be contaminated by adhesive proteins, blood platelets and inflammatory cells in body fluids after being implanted in the body and their anti-adhesive properties can be compromised [20-22]. In addition, pure bactericidal surfaces without an antifouling function will be covered by the remains of dead bacteria, which can facilitate bacterial adhesion, making the situation worse [23-25]. Consequently, bio-inspired antibacterial surfaces, multi-functional composite antimicrobial surfaces and smart antibacterial surfaces that are responsive to the bacterial infection microenvironment have attracted increasing attention.

Many kinds of smart and self-defensive antibacterial coatings or drug delivery systems have been developed in recent years [26-28]. These antibacterial surfaces consist of components that are responsive to pH, temperature, light, enzymes, and even bacterial infections [17, 29, 30]. For example, Jiang *et al*. synthesized a series of zwitterionic polymers that are reversibly switchable between bactericidal and fouling release activities [31]. Sukhishvili *et al*. developed a series of smart multilayer films for antibiotic delivery that are responsive to bacterial infections and show bacteria-triggered and on-demand release properties [17, 28, 32]. The obvious advantage of this drug delivery strategy is the reduction of the uncontrolled and excessive release of antibiotics, which will inhibit the development of resistant bacteria. In our previous studies, we constructed (heparin/chitosan)$_{10}$- (polyvinylpyrrolidone/poly(acrylic acid))$_{10}$ ((HEP/CHI)$_{10}$-(PVP/PAA)$_{10}$) multilayer films based on electrostatic and hydrogen bond interactions [33]. The controlled hydrolysis of the outer (PVP/PAA)$_{10}$ multilayer films through thermal cross-linking resulted in excellent anti-adhesion properties. We also designed and developed self-defensive antibiotic delivery multilayer films with methoxy poly(ethylene glycol)-poly(ε-caprolactone)-chitosan as a drug carrier and assembly component [34]. The local acidic environment of bacterial infections stimulated the antibiotic release from the multilayer films. It has been found that bacterial adhesion and infections often lead to microenvironmental changes such as acidification, and increases in the concentration of specific enzymes (such as hyaluronidase and chymotrypsin) and virulence factors [26, 35, 36].

However, the most commonly used method to control bacterial infections is through oral or intravenously delivered broad-spectrum antibiotics. This is the most effective method of clinical application to prevent bacterial infections[34]. Unfortunately, greater numbers of resistant bacteria have emerged because of the widespread and excessive use of antibiotics. In the present work, we aimed to construct enzymatically degradable (hyaluronic acid/chitosan)$_n$- (hyaluronic acid/polylysine)$_n$ ((HA/CHI)$_n$-(HA/PLL)$_n$) composite multilayer films that are responsive to

View Article Online
DOI: 10.1039/C7TB02114C

hyaluronidase and chymotrypsin for smart bacterial anti-adhesion and bactericidal synergistic functions. The growth behavior and thickness of the multilayer films were explored through spectroscopic ellipsometry and scanning electron microscopy (SEM) cross section measurements. The enzymatic degradation process was specifically studied in the presence of hyaluronidase and chymotrypsin or *Staphylococcus aureus* (*S. aureus*) through a thickness and topography investigation. The antibacterial properties of the material were also examined using an agar plate counting and bacterial LIVE/DEAD staining method both *in vitro* and *in vivo*.

2. Materials and methods

2.1. Materials and reagents

Polydimethylsiloxane (PDMS) was purchased from Dow Corning (Sylgard®184) and made into solid according to the instructions, using 10:1 ratio of elastomer base to curing agent. HA was purchased from Freda Biochem Co., Ltd. Polyethyleneimine (PEI, *Mw*: 25 kDa), Poly-L-lysine hydrobromide (PLL, *Mw*: 4000-15000 by viscosity), Chitosan (CHI, *Mw*: 10 kDa, 75-85% deacetylation), hyaluronidase (HAS, from bovine testes, Type I-S, lyophilized powder, 400-1000 units/mg solid) and chymotrypsin (CMS, α-chymotrypsin from bovine pancreas, Type II, lyophilized powder, ≥40 units/mg protein) were purchased from Sigma-Aldrich.

2.2. Construction of the $(HA/CHI)_{10}$-$(HA/PLL)_{10}$ multilayer films

Substrates such as glass discs, PDMS and silicon wafers were successively cleaned in ethanol, acetone and water before using. CHI in acetic acid and HA in water were dissolved at 1 mg/mL and pH 4.5 for $(HA/CHI)_{10}$ multilayer films deposition, and then PLL and HA were dissolved at pH 6.5 for $(HA/PLL)_{10}$ multilayer films deposition. Substrates were firstly aminated through dipping in PEI solution (5 mg/mL) for 30 min. To construct the $(HA/CHI)_{10}$-$(HA/PLL)_{10}$ multilayer films, the substrates were alternately dipped in HA solution and CHI solution for 10 min and washed in the buffer solution (pH=4.5) until the numbers of bilayers were obtained. Then the $(HA/PLL)_{10}$ multilayer films were immersed alternately in PLL and HA solutions for 10 min with an intermediate rinsing step in buffer solution (pH=6.5). The composite $(HA/CHI)_{10}$-$(HA/PLL)_{10}$ multilayer films were dried under a gentle stream of N_2. This dipping cycle corresponds to the deposition of one bilayer.

2.3. Multilayer films thickness measurement

In the process of multilayer films preparation, the changes of thickness were tracking tested by spectroscopic ellipsometry (M-2000 DITM, J.A. Woollam). This measurement was carried out on silicon wafers. The continuous wave length ranging from 124 to 1700 nm and angle of incidence of both 65º and 70º were chosen for the ellipsometry measurements. Δ and Ψ values measured at wavelength of 600-1700 nm were chosen for data analysis. Cauchy model was applied for determining the thickness of multilayer films. Parameters of A_n and B_n for Cauchy layer were set as 1.45 and 0.01 respectively as fit parameters. Then the thickness that best fit the multilayer films could be automatically calculated. Then the thickness that best fit the multilayer films could be

View Article Online
DOI: 10.1039/C7TB02114C

automatically calculated. SEM (SiRion100) was also used to measure surface morphology and thickness of the multilayer film. When the desired number of the film was deposited, the silicon wafers with the multilayer films were dried and snapped. The cross-sectional images of the multilayer films were obtained to measure the thickness.

2.4. Enzyme and bacterial responsive degradation of the multilayer films

The obtained multilayer films were immerged in HAS/CMS (20/20 U/mL) complex solutions or 10^5 CFU/mL *S. aureus* in 0.01 M PBS for 72 h. The samples were taken out at certain time interval and dried by N_2 for thickness measurement by spectroscopic ellipsometry and SEM (SiRion100) cross section observation. The surface morphology changes of the multilayer films on silicon wafers were also examined by SEM after drying. Surface wettability of the films was measured by Drop Shape Analysis (KRŰSS, DSA10-MK2). The sessile dropping method was used to detect surface of the coatings within 15 s after the ultrapure water droplet contacted the surface. The contact angle formed between the sample surface and droplet was measured using built-in microscope and software provided by manufacturer. The specific surface area and the mean diameter of the multilayer films were determined by N_2 adsorption in accordance to the BET (Brunauer-Emmett-Teller) specific surface area analysis, measured on Micromeritics 3Flex instrument. The BET surface area was determined based on six measurements at relative pressure of N_2 in the range of 0.05-1.00.

2.5. Cytotoxicity assays

The human lens epithelial cells (HLECs, from ATCC, SRA01/04) were grown in DMEM/F12 (1:1) mixed medium supplemented with 10 % fetal bovine serum, 100 U/mL penicillin, and 100 μg/mL streptomycin in a 5 % CO_2 incubator at 37 °C. Confluent cells were digested using 0.25 % trypsin-0.02 % EDTA, followed by centrifugation (1000 g for 3 min) to harvest the cells. Subsequently, the single cell suspension was used for cell number calculation using haemacytometer. After confluence, cells were digested and resuspended for cultivation on the materials. The HLECs were seeded onto the specimens at a density of 1.0×10^4 cells per sample by using 96-well tissue culture plate as the holder, cultivation was conducted for 24 h.

Then, Cell Counting Kit-8 (CCK-8, Beyotime, China) assay was used for the viability studies of cells grown on the resulting multilayer films. After HLECs were inoculated on the multilayer films modified dishes for 24 h, the original medium was replaced by 100 μL 10 % FBS DMEM/F12 (1:1) mixed medium contains 10 μL CCK-8. It was incubated at 37 °C for 2 h to form water dissoluble formazan. Then 100 μL of the above formazan solution were taken from each sample and added to one well of a 96-well plate, six parallel replicates were prepared. The absorbance at 450 nm (calibrated wave) was determined using a microplate reader (Multiskan MK33, Thermo electron corporation, China). Tissue culture plates (TCPS) without any coating were used as a control.

2.6. *In vitro* antibacterial test

Antimicrobial tests of $(HA/CHI)_{10}$-$(HA/PLL)_{10}$ multilayer films were conducted qualitatively and quantitatively by bacterial LIVE/DEAD staining method respectively with *Escherichia coli* (*E.*

View Article Online
DOI: 10.1039/C7TB02114C

coli, ATCC 8739) and *S. aureus* (ATCC 6538) as model bacteria. A LIVE/DEAD BacLight bacterial viability kit (L-7012, Invitrogen) was used to determine bacterial cell viability. This test evaluates the structural integrity of bacterial membrane. The $(HA/CHI)_{10}$-$(HA/PLL)_{10}$ multilayer films modified and control PDMS sheets were incubated with *S. aureus* or *E. coli* for 24 h and stained according to the kit protocol. After careful washing, the samples were sealed with tin foil and observed by fluorescence microscope investigation (Zeiss, Germany).

2.7. Animal experiments of antibacterial activity

The study was approved by the Institutional Animal Care and Use Committee of Wenzhou Medical University. Experiments were carried out in New Zealand white rabbits, weighing between 2.5 and 3.5 kg (obtained from the Animal Administration Center of Wenzhou Medical University). The rabbits were treated in accordance with guidelines set forth by the Association for Research in Vision and Ophthalmology. Four groups of animals were studied for $(HA/CHI)_{10}$, $(HA/PLL)_{10}$ and $(HA/CHI)_{10}$-$(HA/PLL)_{10}$ multilayer films and native PDMS, respectively. All implants were sterilized prior to implantation and stored in sealed Petri dishes.

The animal model used conformed to that described in our previous work[9]. New Zealand White rabbits were anesthetized using isoflorane delivered by facemask. A broad area of the back was shaved, and the underlying skin washed with surgical scrub, wiped with alcohol, painted with betadine, and draped for surgery. Under sterile conditions, two subcutaneous symmetrical multilayer films-coated and uncoated PDMS implants were created on either side of the spine; care was taken to ensure broad physical separation between the implants to eliminate cross-contamination risks. In the rabbits, the subcutaneous pocket was then inoculated with 1 mL of the 10^8 cells/mL *S. aureus* suspension. The incisions were closed in a single layer with 4-0 interrupted nylon suture and the epidermis was cleaned with 2 % H_2O_2. Rabbits were housed individually and given ad libitum access to food and water.

The animals were then observed daily throughout a 1 week period, after which they were returned to the operating room and prepared as above. Each pocket was opened via a small incision distinct from the prior wound, through which two sterile cotton swabs were inserted, sequentially. The animals were then euthanized, and the incision was extended. A closed container containing the implant immersed in 5 mL of solution was vigorously vortexed for 30 s, followed by sonication for 5 min. From the solution, 0.2 mL was plated onto solid agar in triplicate using the spread plate method. After incubating for 24 h, the number of viable bacteria was counted and the results were expressed as mean colony forming units (CFU) per mL. After obtaining culture samples, each pocket was excised en bloc, and transmural sections from representative areas taken. Specimens were fixed in 10% formalin and embedded in paraffin blocks. Tissue sections, 5 mm thick, were mounted onto slides, which were stained using hematoxylin and eosin

Statistical analysis

All experiments were conducted in triplicate, and data points were expressed as the mean. Two sample t test in origin 8.0 (Microcal, USA) were used to compare data obtained with the different samples under identical treatments. A value of $p < 0.05$ was considered significant.

3. Results and discussion

View Article Online
DOI: 10.1039/C7TB02114C

3.1. Construction of the $(HA/CHI)_{10}$-$(HA/PLL)_{10}$ multilayer films

The adhesion of bacteria on an implant surface is an essential step in the development of biofilms and bacterial infections. It has been demonstrated in previous studies that controlled erasable films coated on the implants could almost completely resist bacterial adhesion within a certain period of time [33, 37]. In order to enhance the specificity and efficiency of the response of modified films to the bacterial infection microenvironment, enzyme responsive degradable multilayer films were designed and constructed for both short-term bacterial adhesion resistance and long-term biofilm inhibition [38, 39]. Bacterial infections lead to a significant increase in the levels of enzymes such as HAS and CMS in the microenvironment around the implants. As a result, PLL and HA were chosen as assembly components which could be enzymatically degraded by CMS and HAS, respectively. In addition, the polycation PLL and CHI possess effective antibacterial properties.

As shown in Figure 1, composite multilayer films were successively assembled on PEI aminated substrates. Both the PLL and HA components in the top $(HA/PLL)_n$ multilayer films could be enzymatically degraded in the presence of CMS and HAS or bacteria that could secrete these two kinds of enzymes. However, for the bottom $(HA/CHI)_n$ multilayer films, the blocking effect of CHI could reduce the enzymatic degradation rate of HA by HAS. Afterwards, the exposed $(HA/CHI)_{10}$ multilayer films also exert a bactericidal function against bacteria through contact killing. Furthermore, the complete degradation time of the $(HA/PLL)_n$ multilayer films could be tuned through changing the number of bilayers. In addition, the high water content of the $(HA/CHI)_n$ multilayer films could endow them with significant hydrophilic properties to resist bacterial adhesion.

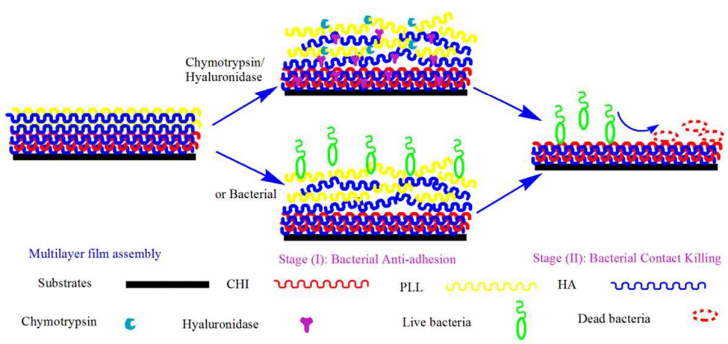

Figure 1. Schematic representation of the $(HA/CHI)_n$-$(HA/PLL)_n$ self-assembled multilayer films and the enzyme-triggered and bacteria-triggered degradation of the films.

View Article Online
DOI: 10.1039/C7TB02114C

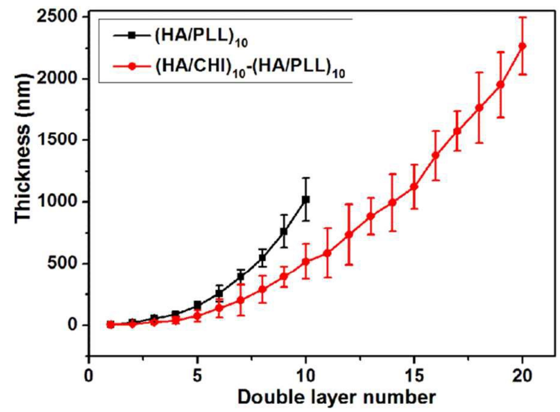

Figure 2. Ellipsometry measurement of the $(HA/PLL)_{10}$ and $(HA/CHI)_{10}$-$(HA/PLL)_{10}$ multilayer films.

The $(HA/CHI)_n$ and $(HA/PLL)_n$ multilayer films demonstrate two kinds of rapid exponential growth owing to the polycation "in and out" diffusion mechanism or the rapid increase of surface roughness. In the present work, the ellipsometry measurements in Figure 2 demonstrate the exponential growth characteristics of the $(HA/PLL)_{10}$ and $(HA/CHI)_{10}$-$(HA/PLL)_{10}$ multilayer films. The "in and out" diffusion of the PLL component should be the mechanism of the exponential growth of the $(HA/PLL)_n$ multilayer films. The thickness of the obtained $(HA/PLL)_{10}$ and $(HA/CHI)_{10}$ multilayer films was 1019.7 ± 172.2 nm and 519.6 ± 142.6 nm, respectively. Then $(HA/PLL)_{10}$ multilayer films were also constructed on $(HA/CHI)_{10}$ multilayer films showing a faster growth rate, which could be attributed to both "in and out" diffusion and an increase in surface roughness composite mechanisms. The thickness rapidly increased from 519.6 ± 142.6 nm to 2265.6 ± 231.4 nm after the deposition of $(HA/PLL)_{10}$ multilayer films, which was beneficial in achieving long-term resistance to bacterial adhesion through enzymatic degradation.

3.2. Enzyme and bacterial responsive degradation of the multilayer films

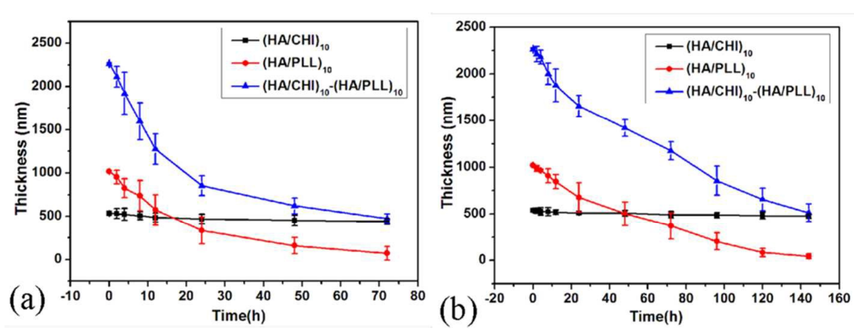

Figure 3. Thickness changes of the multilayer film (a) in HAS/CMS (20/20 U/mL) composite enzyme solutions and (b) in 10^5 CFU/mL *S. aureus* solution as measured by ellipsometry.

View Article Online
DOI: 10.1039/C7TB02114C

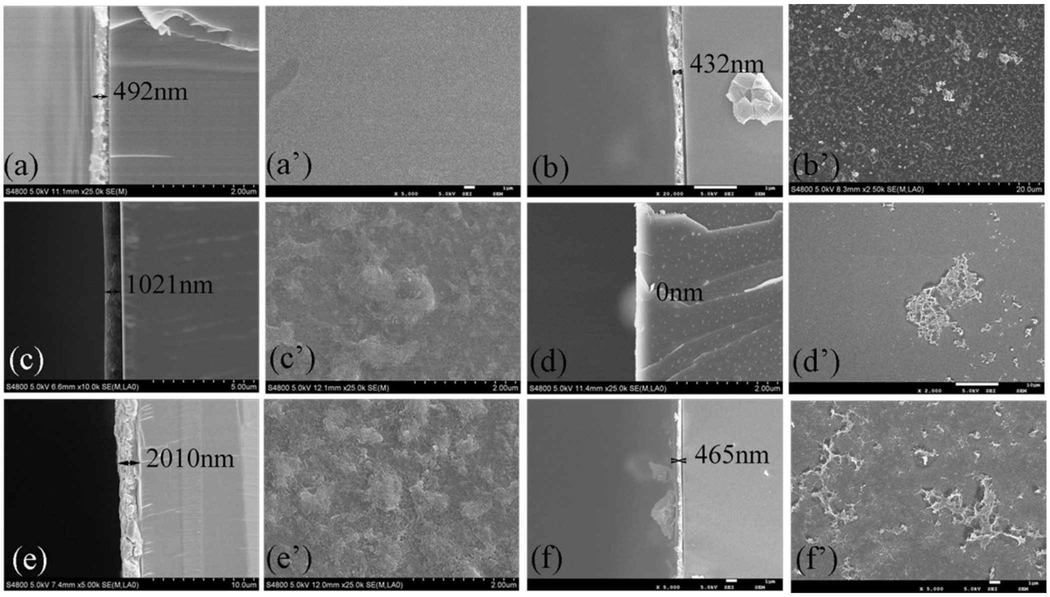

Figure 4. Thickness and surface morphology changes of (a, a', b, b') $(HA/CHI)_{10}$, (c, c', d, d') $(HA/PLL)_{10}$ and (e, e', f, f') $(HA/CHI)_{10}$-$(HA/PLL)_{10}$ multilayer films before and after being immersed in HAS/CMS (20/20 U/mL) composite enzyme solutions for 72h as measured by SEM.

In order to investigate the enzyme and bacteria responsive degradation of the $(HA/CHI)_{10}$-$(HA/PLL)_{10}$ multilayer films, the film thickness and internal structure changes were assessed using spectroscopic ellipsometry, water contact angle (WCA), BET and SEM. As shown in Figure 3, the degradation profiles were similar for the obtained multilayer films in HAS/CMS composite enzyme solutions or 10^5 CFU/mL *S. aureus*. As indicated in Figure 3a and Figure 4a, 4a', 4b, and 4b', after immersion in HAS/CMS (20/20 U/mL) complex solutions for 72 h, the thickness of the $(HA/CHI)_{10}$ multilayer films decreased from 507.7 ± 29.4 nm to 442.4 ± 34.2 nm. The WCA changed from 68.3±4.6º to 45.4±7.1º indicating the rapid spreading and permeating of water on the films. BET specific surface area of the multilayer films increased from 0.3 into 4.3 m^2/cm^2 also proved the porous structure after degradation. The surface morphology changed from smooth and uniform to rough and uneven indicating the serious enzymatic degradation of HA by HAS. As shown in Figure 4b, a large number of pore structures emerged throughout the films after 72 h of degradation, as assessed using a SEM cross section observation. The degradation rate in *S. aureus* was much slower than that in HAS/CMS and the thickness decreased to 476.7 ± 24.5 nm after immersion for 144 h (Figure 3b). It has been reported that the enzyme concentration has a great effect on the degradation of the films. Freestanding $(HA/CHI)_{10}$ multilayer films constructed by Cardoso *et al*. exhibited accelerated weight loss up to 120 h and completed the degradation after 14 d in the presence of 50 µg/mL (~250 U/mL) of HAS [40].

As for the $(HA/PLL)_{10}$ multilayer films, the thickness rapidly decreased from 1019.7 ± 17 nm to 336.5 ± 156 nm in the first 24 h and they were almost completely degraded after 72 h. Both the HA and PLL components could be degraded by HAS and CMS, leading to the rapid degradation of the multilayer films. As observed in Figure 4c, 4c', 4d and 4d', the surface of the $(HA/PLL)_{10}$ multilayer films was quite rough, which contributed to the exponential growth of the films. There was only some residual degraded film on the surface of the silicon wafers indicating the complete

View Article Online
DOI: 10.1039/C7TB02114C

degradation of the films. The degradation rate of the $(HA/PLL)_{10}$ multilayer films was much slower in *S. aureus* solution and the thickness decreased to 676.6 ± 156.1 nm at 24 h and 371.7 ± 141.4 nm at 48 h, and the films were almost totally degraded by 144 h. The $(PLL/HA)_{18}$ multilayer films (1.8 μm) on glass substrates prepared by Kadi *et al*. showed HAS concentration dependent degradation and rapidly degraded in the first 3 d [41].

For the $(HA/CHI)_{10}$-$(HA/PLL)_{10}$ multilayer films, the surface roughness was much higher than that of the $(HA/PLL)_{10}$ multilayer films, as shown in Figure 4e and 4e'. The degradation rate was rapid in the first 24 h (from 2265.6 ± 114.2 nm to 854.4 ± 112.6 nm) and the thickness gradually decreased to 476.3 ± 56.3 nm at 72 h. Figure 4f and 4f' display the total degradation of the top $(HA/PLL)_{10}$ multilayer films leaving some remains on the surface. The changing of WCA from 52.1±3.8º to 65.3±6.3º showed fully degradation of $(HA/PLL)_{10}$ multilayer films. BET specific surface area of the multilayer films increased from 0.3 into 0.8 m^2/cm^2 also proved the porous structure of the remaining $(HA/CHI)_{10}$ multilayer films. It was obvious that the degradation rate of the multilayer films in the *S. aureus* suspension was much lower than that in HAS/CMS solutions. The HAS concentration in human serum is of the order of 2.6 U/mL [42], and the concentration increases significantly in the presence of bacterial infections. It can be concluded that the presence of both HAS and CMS accelerated the degradation of the top $(HA/PLL)_{10}$ multilayer film. The successive degradation of the films and the detaching of the film fragments would efficiently reduce bacterial adhesion. It is predicated that with the passage of time the remaining bottom $(HA/CHI)_{10}$ multilayer films will gradually be enzymatically degraded by HAS leading to the inhibition of biofilm formation on the implant surface [40].

3.3. Cytotoxicity evaluation

In this system, all the components, including HA, CHI and PLL have good biocompatibility against mammalian cells. However, as polycations, CHI and PLL may possess low cytotoxicity [43, 44]. This was investigated using HLECs as model cells through a viability evaluation. As shown in Figure 5, the glass discs had nearly no cytotoxicity compared with TCPS. There was not much difference in the cell inhibitory activities of the $(HA/CHI)_{10}$, $(HA/PLL)_{10}$ and $(HA/CHI)_{10}$-$(HA/PLL)_{10}$ multilayer films, which were significantly higher than that of the glass discs and TCPS ($p<0.05$). The antibacterial mechanism of the polycations could be attributed to the electrostatic interactions of the NH_3^+ with the negatively charged cell surface and a subsequent change in membrane permeability, leading to the leakage of intracellular components and bacterial cell death [43, 45]. This process could also cause cytotoxicity against HLECs.

View Article Online
DOI: 10.1039/C7TB02114C

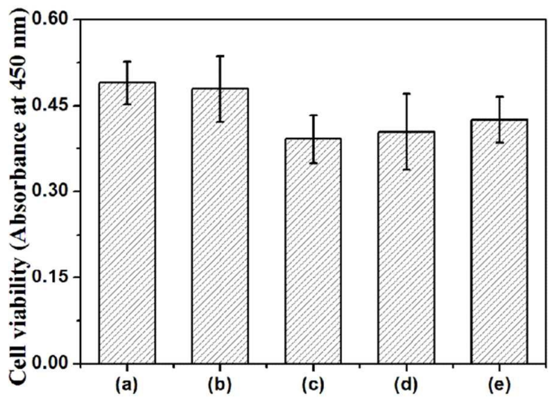

Figure 5. The cell viability assay of HLECs cultured on the surfaces of (a) TCPS, (b) pristine PDMS, (c) $(HA/CHI)_{10}$, (d) $(HA/PLL)_{10}$ and (e) $(HA/CHI)_{10}$-$(HA/PLL)_{10}$ multilayer films after incubation for 24 h

3.4. Antibacterial and biofilm inhibition properties

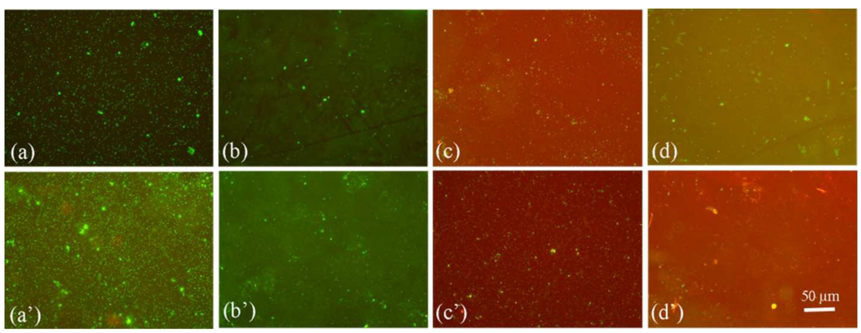

Figure 6. Fluorescent microscopy images of live/dead staining of *S. aureus* adhesions on (a, a') pristine PDMS, (b, b') $(HA/CHI)_{10}$, (c, c') $(HA/PLL)_{10}$ and (d, d') $(HA/CHI)_{10}$-$(HA/PLL)_{10}$ multilayer films modified PDMS, respectively, after 4 h or 72 h of exposure (the magnification was 10×).

The Live/Dead BacLight Bacterial Viability Kit contains two nucleic stains, SYTO 9 and propidium iodide (PI), and is usually used to qualitatively and quantitatively explore bacterial adhesion and activities on biomaterial surfaces [46]. The cell membranes of live bacteria can be permeated by SYTO 9 and the DNA will be stained to exhibit green fluorescence. The destroyed membrane of dead bacteria can be labeled using PI to exhibit red fluorescence. The $(HA/CHI)_{10}$, $(HA/PLL)_{10}$ and $(HA/CHI)_{10}$-$(HA/PLL)_{10}$ multilayer films were incubated with 1×10^5 CFU/mL *S. aureus* or *E. coli* for 4 h or 24 h and stained using a combination dye of SYTO 9/PI according to the kit protocol. As shown in Figure 6a, 6a' and Figure 7a, 7a', there were numerous distinguishable bacteria stained green on the PDMS indicating the absence of anti-adhesion and bactericidal activity on the PDMS surface at 4 h. With the growth of the adhered bacteria, the PDMS surface was almost covered by a bacterial layer demonstrating green fluorescence at 72 h and this was the initial stage of a biofilm.

However, the numbers of *S. aureus* and *E. coli* on the $(HA/PLL)_{10}$ multilayer films were much less than those on the PDMS, which demonstrated the excellent bacterial anti-adhesion activity of

View Article Online
DOI: 10.1039/C7TB02114C

the $(HA/PLL)_{10}$ multilayer films (Figure 6b, 6b' and Figure 7b, 7b'). As observed in Figure 3, the $(HA/PLL)_{10}$ multilayer films could be rapidly enzymatically degraded in the initial 24 h which caused the detachment of bacteria from the surface. However, the film was lacking a bactericidal function against bacteria and the adhered *S. aureus* and *E. coli* were stained green. Compared with gram-negative *E. coli*, gram-positive *S. aureus* colonize the films much more easily and their proliferation ability was much stronger than that of *E. coli*. As for the $(HA/CHI)_{10}$ multilayer films, their bactericidal properties were quite significant at 4 h (Figure 6c and Figure 7c) and most of the adhered bacteria had been killed and exhibited red fluorescence when stained. The presence of CHI in the films might be the main reason for the high contact killing properties of the $(HA/CHI)_{10}$ multilayer films [47-49]. However, the number of live bacteria stained green gradually increased after incubation with bacteria for 24 h (Figure 6c' and Figure 7c'). This can be attributed to the appearance of porous structures and the significant increase of the surface roughness, which compromised the anti-adhesion properties as the enzymatic degradation rate was rather slow (Figure 4b and 4b').

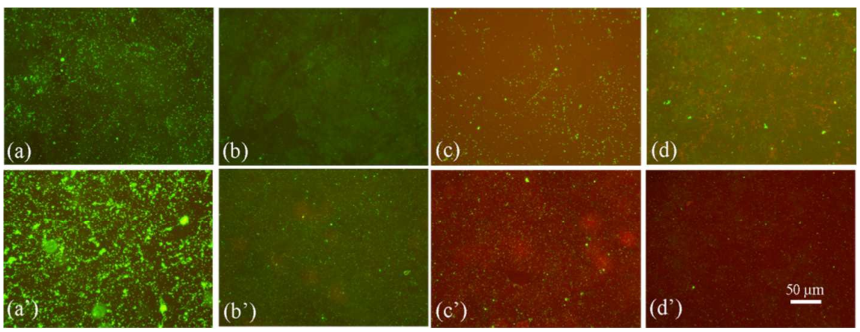

Figure 7. Fluorescent microscopy images of live/dead staining of *E. coli* adhesions on (a, a') pristine PDMS, (b, b') $(HA/CHI)_{10}$, (c, c') $(HA/PLL)_{10}$ and (d, d') $(HA/CHI)_{10}$-$(HA/PLL)_{10}$ multilayer films modified PDMS, respectively, after 4 h or 72 h of exposure (the magnification was 10×).

In comparison with the $(HA/CHI)_{10}$ and $(HA/PLL)_{10}$ multilayer films, the $(HA/CHI)_{10}$-$(HA/PLL)_{10}$ multilayer films showed ideal antibacterial properties. In the first 4 h, the degradation of the top $(HA/PLL)_{10}$ multilayer film led to the adhesion resistance of the surface and there were only a few cells (stained green) sparsely distributed on the multilayer films (Figure 6d and Figure 7d). After 144 h of degradation in the bacterial infection microenvironment, the top $(HA/PLL)_{10}$ multilayer films had been almost totally degraded by enzymes secreted by the bacteria (Figure 4f and 4f'). The exposed $(HA/CHI)_{10}$ multilayer films still exhibited good bactericidal properties against *S. aureus* and *E. coli*. In addition, the total degradation time of the top $(HA/PLL)_{10}$ multilayer films can be controlled through regulating the thickness and the bilayer number of the top multilayer films. This kind of self-dissolving antibacterial coating on the implants is especially suited for use in catheters, stents and orthopedic implants that can easily be contaminated by proteins, bacteria, inflammatory cells and inorganic material. The composite $(HA/CHI)_{10}$-$(HA/PLL)_{10}$ multilayer films possess obvious advantages in their comprehensive antibacterial performance compared with the pure $(HA/CHI)_{10}$ and $(HA/PLL)_{10}$ multilayer films.

To our knowledge, the long-term should be 5-7 days or even longer time. The first 24 h after an implantation of a biomedical device has been considered as a "decisive period", during which microbes can easily adhere and colonize on implants. The reason could be the compromised

View Article Online
DOI: 10.1039/C7TB02114C

immune system of patients whose defensive cells show weak bactericidal activities. Prevention of microbes' adhesion during this decisive period is critical and can thus significantly increase the long-term success rate of biomedical implants. As a result, For the $(HA/CHI)_{10}$-$(HA/PLL)_{10}$ multilayer films were designed and constructed for both short-term bacterial resistance and long-term biofilm inhibition property. The successive degradation of the films and the detaching of the film fragments would efficiently reduce bacterial adhesion. The exposed $(HA/CHI)_{10}$ multilayer films still exhibited good bactericidal properties against *S. aureus* and *E. coli* (Figure 6 and7).

3.5. Antibacterial activity *in vivo*

A bacterial infection model in rabbits was used to investigate the *in vivo* antibacterial properties of the multilayer films, which were inoculated using 10^8 CFU/mL *S. aureus* [50]. After 7 d incubation, the implants were removed from the cavities for SEM observation or washed in an ultrasonicator using phosphate buffered saline for agar plate counting (Figure 8). There was a clear difference in terms of bacterial adhesion on the different surfaces. There were lots of *S. aureus* cells covering the PDMS and most of the bacteria were live, indicating a serious infection (Figure 8a and 8a'). However, the numbers of bacteria on the three kinds of multilayer film were much less than those on the PDMS. The anti-adhesion properties of the films could be attributed to their high swelling performance together with their long-term enzymatic degradation in a bacterial infection microenvironment. Moreover, the number of live *S. aureus* on the $(HA/CHI)_{10}$ multilayer films was higher than that on the $(HA/PLL)_{10}$ and the $(HA/CHI)_{10}$-$(HA/PLL)_{10}$ multilayer films, which could be caused by the absence of enzymatic degradation properties (as shown in Figure 3 and 4).

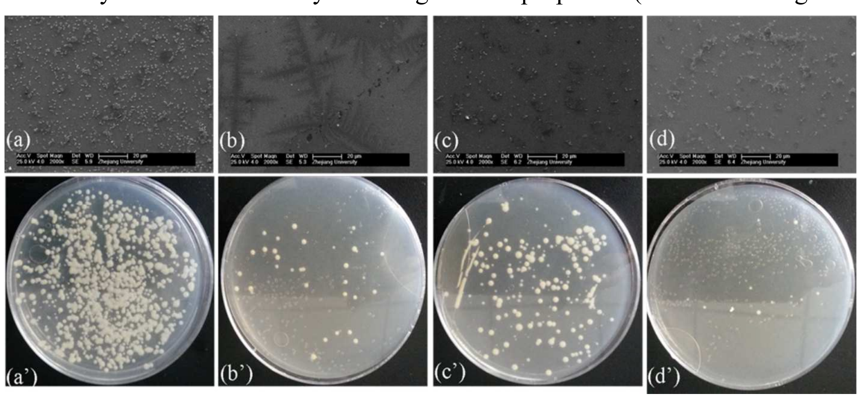

Figure 8. SEM images of *S. aureus* adhesion and agar plate counting on (a, a') pristine PDMS, (b, b') $(HA/CHI)_{10}$, (c, c') $(HA/PLL)_{10}$ and (d, d') $(HA/CHI)_{10}$-$(HA/PLL)_{10}$ multilayer films modified PDMS, respectively, after 7 d incubation in the rabbits

View Article Online
DOI: 10.1039/C7TB02114C

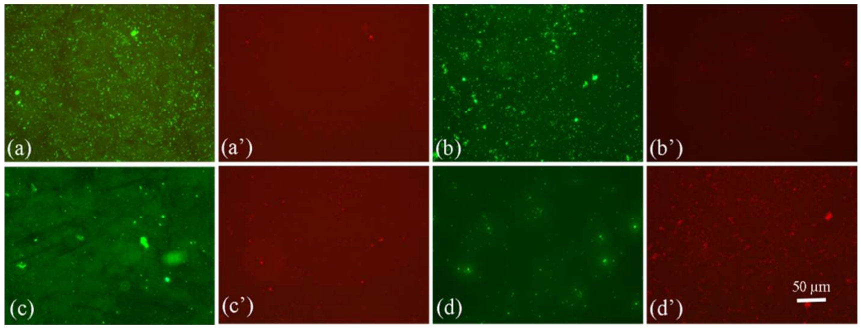

Figure 9. Fluorescent microscopy images of live/dead staining of *S. aureus* adhesions on F(a, a') pristine PDMS, (b, b') $(HA/CHI)_{10}$, (c, c') $(HA/PLL)_{10}$ and (d, d') $(HA/CHI)_{10}$-$(HA/PLL)_{10}$ multilayer films modified PDMS, respectively, after 7 d incubation in the rabbits

The bacterial cell viability was also determined through a bacterial live/dead staining method using the LIVE/DEAD BacLight bacterial viability kit. The PDMS and $(HA/PLL)_{10}$ multilayer films showed no bactericidal function against *S. aureus* which exhibited green fluorescence once stained. A uniform bacterial layer formed on the surface of the PDMS which was the initial stage of a biofilm. The reason why there was a lot of bacteria on the $(HA/PLL)_{10}$ multilayer films was that after a 7 d implantation the films had nearly been completely degraded by the HAS and CMS secreted by the bacteria. In contrast, there were much fewer bacteria, stained either red or green, on the $(HA/CHI)_{10}$ and the $(HA/CHI)_{10}$-$(HA/PLL)_{10}$ multilayer films. Although it was demonstrated in the *in vitro* antibacterial test that many bacteria adhered on the $(HA/CHI)_{10}$ multilayer films, there were few bacteria dispersed on the films *in vivo*. This phenomenon can be ascribed to the complexity of the *in vivo* environment, which enhanced the enzymatic degradation rate of the multilayer films. Bacterial proliferation and enzyme secretion would have been more rapid in the *in vivo* environment. In addition, other kinds of enzymes, such as chitosanase, might contribute to the degradation of the films. In summary, the $(HA/CHI)_{10}$-$(HA/PLL)_{10}$ multilayer films demonstrated not only the best anti-adhesive properties, but also the best contact killing activity in *in vivo* antibacterial tests.

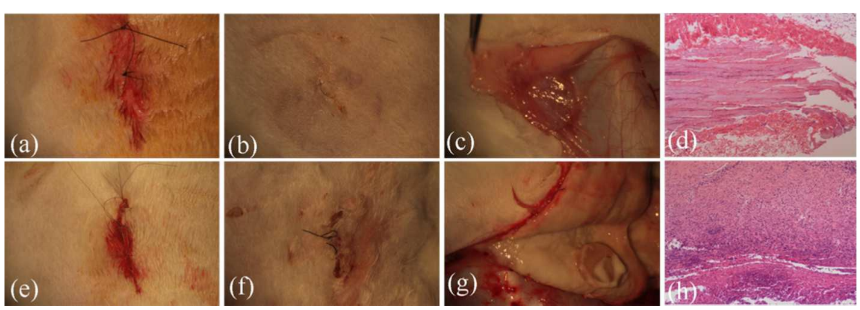

Figure 10. Photographs of pockets after operation, at day 7, opened at day 7 and images of hematoxylin and eosin-stained sections of surrounding connective tissues of (a, b. c, d) $(HA/CHI)_{10}$-$(HA/PLL)_{10}$ multilayer films modified PDMS and (e, f, g, h) pristine PDMS.

The appearance of the wounds was recorded just after implantation with either the $(HA/CHI)_{10}$-$(HA/PLL)_{10}$ multilayer films or pure PDMS, and just before the implants were harvested (Figure 10a, 10b, 10e and 10f). It was found that the wounds implanted with film-coated

View Article Online
DOI: 10.1039/C7TB02114C

PDMS healed better than those implanted with pure PDMS. After the implants were harvested, an exuberant purulent discharge was found in seven of eight PDMS-implanted wounds indicating the presence of serious bacterial infections. However, the wounds with film-coated implants were free of purulent discharge and only one of these wounds demonstrated an obvious infection. The adhesion of bacteria on the implants is the first but the most decisive process leading to bacterial growth and biofilm formation. Once the implant surface is colonized and compounded with proteins, polysaccharides and other extracellular matrix components, the bacteria can easily escape from the immune system and antibiotic treatment. As a result, serious bacterial infections occurred in the wounds implanted with pure PDMS. Hematoxylin and eosin stained sections of the tissues adhering to the implants were investigated to examine the tissue response to the implants after 7 d incubation. As shown in Figure 10, there were mild signs of inflammation with a small number of inflammatory cells in the tissues surrounding the antibacterial coating-modified PDMS (Figure 10d). However, there were significantly more inflammatory cells in the tissues adhering to the pure PDMS implant which confirmed the occurrence of an acute inflammatory response. This situation was consistent with the appearance of the wound and the internal amount of purulence. These results demonstrate the antibacterial function of the material *in vivo* and the good biocompatibility of the composite multilayer films. To construct antibacterial surfaces, the self-assembled multilayer films can be used as a multifunctional platform. It is a simple and versatile way to fabricate LBL films on virtually any substrates which involves alternate deposition of polymers with complementary non-covalent interactions. As a consequence, the $(HA/CHI)_n$-$(HA/PLL)_n$ composite multilayer films can be easily constructed on the implants or devices. There are also some alternative approaches to prepare multilayer films on biomaterials such as spraying LBL method.

4. Conclusions

In the present work, $(HA/CHI)_n$-$(HA/PLL)_n$ composite multilayer films were constructed *via* a layer-by-layer self-assembly method and demonstrated exponential growth behavior as measured by spectroscopic ellipsometry and SEM. The top $(HA/PLL)_n$ multilayer films were totally enzymatically degraded in HAS/CMS complex solutions or a bacterial infection microenvironment. A cell activity evaluation demonstrated the low cytotoxicity and good cell compatibility of the multilayer films against HELCs. *In vitro* antibacterial measurements, through bacterial live/dead staining, demonstrated the excellent anti-adhesion properties of the films, through enzymatic degradation of the top multilayer films and their effective bactericidal function against both *S. aureus* and *E. coli*. The effective anti-infection properties of the composite multilayer films were also confirmed through a bacterial infection model in New Zealand white rabbits. The antibacterial coating-modified implants yielded a much lower infection incidence than unmodified implants through the self-defense degradation mechanism, which was responsive to the bacterial infection microenvironment. In summary, the current work provides a novel and smart approach to modify biomaterials, and in particular implants, for synergistic long-term anti-adhesive and biofilm inhibition properties.

Acknowledgements

View Article Online
DOI: 10.1039/C7TB02114C

The National Natural Science Foundation of China (31771026, 51403158, 81771984, 21601139), National Key R&D Program (2016YFC1101201), Zhejiang Natural Science Foundation of China (21601139) and Science & Technology Program of Wenzhou (Y20160068, Y20160058, Y20160061) are greatly acknowledged.

References

1. B. L. Wang, Z. Ye, Y. H. Tang, Y. M. Han, Q. K. Lin, H. H. Liu, H. Chen and K. H. Nan, *International Journal of Nanomedicine*, 2017, **12**, 111-125.
2. G.-A. Junter, P. Thebault and L. Lebrun, *Acta Biomaterialia*, 2016, **30**, 13-25.
3. A. Cochis, B. Azzimonti, C. Della Valle, E. De Giglio, N. Bloise, L. Visai, S. Cometa, L. Rimondini and R. Chiesa, *Biomaterials*, 2016, **80**, 80-95.
4. C. Traba and J. F. Liang, *J Control Release*, 2015, **198**, 18-25.
5. B. L. Wang, Y. M. Han, Q. K. Lin, H. H. Liu, C. H. Shen, K. H. Nan and H. Chen, *Journal of Materials Chemistry B*, 2016, **4**, 1853-1861.
6. C. M. Tilmaciu, M. Mathieu, J. P. Lavigne, K. Toupet, G. Guerrero, A. Ponche, J. Amalric, D. Noel and P. H. Mutin, *Acta Biomaterialia*, 2015, **15**, 266-277.
7. B. L. Wang, T. W. Jin, Y. M. Han, C. H. Shen, Q. Li, Q. K. Lin and H. Chen, *Journal of Materials Chemistry B*, 2015, **3**, 5501-5510.
8. B. L. Wang, H. H. Liu, Z. F. Wang, S. Shi, K. H. Nan, Q. W. Xu, Z. Ye and H. Chen, *Journal of Materials Chemistry B*, 2017, **5**, 1498-1506.
9. Q. W. Xu, H. H. Liu, Z. Ye, K. H. Nan, S. Lin, H. Chen and B. L. Wang, *Carbohydrate Polymers*, 2017, **161**, 53-62.
10. X. Q. Dou, D. Zhang, C. L. Feng and L. Jiang, *Acs Nano*, 2015, **9**, 10664-10672.
11. B. L. Wang, Q. K. Lin, T. W. Jin, C. H. Shen, J. M. Tang, Y. M. Hana and H. Chen, *Rsc Advances*, 2015, **5**, 3597-3604.
12. C. R. Arciola, D. Campoccia, P. Speziale, L. Montanaro and J. W. Costerton, *Biomaterials*, 2012, **33**, 5967-5982.
13. B. L. Wang, T. W. Jin, Y. M. Han, C. H. Shen, Q. Li, J. M. Tang, H. Chen and Q. K. Lin, *International Journal of Polymeric Materials and Polymeric Biomaterials*, 2016, **65**, 55-64.
14. B. Wang, Q. Xu, Z. Ye, H. Liu, Q. Lin, K. Nan, Y. Li, Y. Wang, L. Qi and H. Chen, *ACS Appl Mater Interfaces*, 2016, **8**, 27207-27217.
15. B. L. Wang, Z. Ye, Y. H. Tang, H. H. Liu, Q. K. Lin, H. Chen and K. H. Nan, *Journal of Physical Chemistry C*, 2016, **120**, 6145-6155.
16. A. Perez-Anes, M. Gargouri, W. Laure, H. Van Den Berghe, E. Courcot, J. Sobocinski, N. Tabary, F. Chai, J. F. Blach, A. Addad, P. Woisel, D. Douroumis, B. Martel, N. Blanchemain and J. Lyskawa, *Acs Applied Materials & Interfaces*, 2015, **7**, 12882-12893.
17. Y. M. Lu, Y. Wu, J. Liang, M. R. Libera and S. A. Sukhishvili, *Biomaterials*, 2015, **45**, 64-71.
18. Q. Yu, Z. Q. Wu and H. Chen, *Acta Biomaterialia*, 2015, **16**, 1-13.
19. C. J. Huang, Y. S. Chen and Y. Chang, *Acs Applied Materials & Interfaces*, 2015, **7**, 2415-2423.
20. J. Bergek, M. A. Trojer, H. Uhr and L. Nordstierna, *J Control Release*, 2016, **225**, 31-39.
21. H. Lee, J. B. Gilbert, F. E. Angile, R. Yang, D. Lee, M. F. Rubner and R. E. Cohen, *Acs Applied Materials & Interfaces*, 2015, **7**, 1004-1011.
22. R. Fateh, R. Dillert and D. Bahnemann, *Acs Applied Materials & Interfaces*, 2014, **6**, 2270-2278.

View Article Online
DOI: 10.1039/C7TB02114C

23. B. L. Wang, Z. Ye, Q. W. Xu, H. H. Liu, Q. K. Lin, H. Chen and K. H. Nan, *Biomaterials Science*, 2016, **4**, 1731-1741.
24. W. J. Yang, K. G. Neoh, E. T. Kang, S. L. M. Teo and D. Rittschof, *Progress in Polymer Science*, 2014, **39**, 1017-1042.
25. J. Hasan, R. J. Crawford and E. P. Lvanova, *Trends in Biotechnology*, 2013, **31**, 31-40.
26. G. Cado, R. Aslam, L. Seon, T. Garnier, R. Fabre, A. Parat, A. Chassepot, J. C. Voegel, B. Senger, F. Schneider, Y. Frere, L. Jierry, P. Schaaf, H. Kerdjoudj, M. H. Metz-Boutigue and F. Boulmedais, *Advanced Functional Materials*, 2013, **23**, 4801-4809.
27. C. Traba and J. Liang, *J Control Release*, 2015, **213**, E47-E47.
28. I. Zhuk, F. Jariwala, A. B. Attygalle, Y. Wu, M. R. Libera and S. A. Sukhishvili, *Acs Nano*, 2014, **8**, 7733-7745.
29. C. Picart, A. Schneider, O. Etienne, J. Mutterer, P. Schaaf, C. Egles, N. Jessel and J. C. Voegel, *Advanced Functional Materials*, 2005, **15**, 1771-1780.
30. S. Wu, A. Buthe, H. Jia, M. Zhang, M. Ishii and P. Wang, *Biotechnology and Bioengineering*, 2013, **110**, 1805-1810.
31. Z. Q. Cao, L. Mi, J. Mendiola, J. R. Ella-Menye, L. Zhang, H. Xue and S. Y. Jiang, *Angew Chem Int Edit*, 2012, **51**, 2602-2605.
32. S. Pavlukhina, Y. Lu, A. Patimetha, M. Libera and S. Sukhishvili, *Biomacromolecules*, 2010, **11**, 3448-3456.
33. B.-l. Wang, K.-f. Ren, H. C. J.-l. Wang and J. Ji, *Acs Applied Materials & Interfaces*, 2013, **5**, 4136-4143.
34. H. L. Bailiang Wang, Zefeng Wang, Shuai Shi, Kaihui Nan, Qingwen Xu, Zi Ye and Hao Chen, *Journal of Materials Chemistry B*, 2017, **5**, 9.
35. J. E. Bean, D. R. Alves, M. Laabei, P. P. Esteban, N. T. Thet, M. C. Enright and A. T. A. Jenkins, *Chem Mater*, 2014, **26**, 7201-7208.
36. A. E. Clatworthy, E. Pierson and D. T. Hung, *Nat. Chem. Biol.*, 2007, **3**, 541-548.
37. D. J. Schmidt and P. T. Hammond, *Chemical Communications*, 2010, **46**, 7358-7360.
38. J. Huang, Q. Shu, L. Y. Wang, H. Wu, A. Y. Wang and H. Mao, *Biomaterials*, 2015, **39**, 105-113.
39. J. F. Mano, *Advanced Engineering Materials*, 2008, **10**, 515-527.
40. M. J. Cardoso, S. G. Caridade, R. R. Costa and J. F. Mano, *Biomacromolecules*, 2016, **17**, 1347-1357.
41. S. Kadi, D. Cui, E. Bayma, T. Boudou, C. Nicolas, K. Glinel, C. Picart and R. Auzely-Velty, *Biomacromolecules*, 2009, **10**, 2875-2884.
42. J. B. Leach, K. A. Bivens, C. W. Patrick and C. E. Schmidt, *Biotechnology and Bioengineering*, 2003, **82**, 578-589.
43. B.-l. Wang, J.-l. Wang, D.-d. Li, K.-f. Ren and J. Ji, *Applied Surface Science*, 2012, **258**, 7801-7808.
44. K. Manabe, K. H. Kyung and S. Shiratori, *Acs Applied Materials & Interfaces*, 2015, **7**, 4763-4771.
45. M. Dash, F. Chiellini, R. M. Ottenbrite and E. Chiellini, *Progress in Polymer Science*, 2011, **36**, 981-1014.
46. B. L. Wang, H. H. Liu, B. J. Zhang, Y. M. Han, C. H. Shen, Q. K. Lin and H. Chen, *Colloids and Surfaces B-Biointerfaces*, 2016, **141**, 483-490.

View Article Online
DOI: 10.1039/C7TB02114C

47. F. Costa, S. Maia, J. Gomes, P. Gomes and M. C. L. Martins, *Acta Biomaterialia*, 2014, **10**, 3513-3521.
48. M. Burkatovskaya, G. P. Tegos, E. Swietlik, T. N. Demidova, A. P. Castano and M. R. Hamblin, *Biomaterials*, 2006, **27**, 4157-4164.
49. X. F. Hu, K. G. Neoh, Z. L. Shi, E. T. Kang, C. Poh and W. Wang, *Biomaterials*, 2010, **31**, 8854-8863.
50. B. L. Wang, T. W. Jin, Q. W. Xu, H. H. Liu, Z. Ye and H. Chen, *Bioconjugate Chem*, 2016, **27**, 1305-1313.